

Analysis of Marginal Carbon Intensities in Constrained Power Networks

Pablo A. Ruiz
paruiz@ieee.org

Aleksandr Rudkevich
arudkevich@crai.com

Charles River Associates

Abstract

Jurisdictions across the globe are implementing CO₂ emissions reduction policies. These policies typically ignore most locational issues, probably because the consequences of greenhouse gas emissions do not depend on the exact emission location. However, the response to emission policies and the costs and effectiveness of emissions reduction in power systems are locational in nature. This paper analyzes marginal CO₂ emissions in constrained power networks. Numerical results illustrate the high locational dependence of marginal carbon intensities, and support the need for a more detailed consideration of locational effects in emission reduction policies.

1. Introduction

In an effort to curb and reduce greenhouse gas emissions, jurisdictions across the globe have implemented or are contemplating CO₂ reduction policies. Due to the magnitude of CO₂ emissions from fossil-fueled power generation [1], many CO₂ reduction programs are specifically targeted to the power industry, such as Renewable Portfolio Standards [2] and the Regional Greenhouse Gas Initiative [3]. As a result, the investment and power communities are expressing an increasing interest in the massive deployment of carbon-free technologies, such as wind and solar generation, in the construction of transmission lines to deliver renewable energy to the markets, and in load reduction programs.

The emission of greenhouse gases into the atmosphere is a global problem. When a unit of CO₂ is released into the air, to a large extent the exact geographic location, and to some extent the time, of this event makes little difference on its consequences. In contrast, time and geographical location may make a significant difference in the economic efficiency of actions directly or indirectly focused on reduction in CO₂ emissions. This is especially true for the power industry, where a diverse technological and geographical mix of generation technologies and a constrained transmission network make avoidance of CO₂ emissions to be temporally and spatially dependent [4], [5]. In spite of this,

most emission reduction programs do not explicitly account for network or time effects. In fact, there seems to be a disconnect between the great level of detail employed in the economic modeling, simulation and analysis of the effects of new policies, programs and investments [6], [7] compared to a relatively poor system of concepts addressing the implications of CO₂ abatement policies for the economics and operation of power systems.

To improve the understanding of CO₂ emissions economics, this paper defines several sensitivity indicators specifically addressing the economics of carbon¹ emissions within the operation of a power system. The *marginal nodal carbon intensity* of a specified node is defined as the decrease in CO₂ emissions in the electrical network in response to an infinitesimal decrease in electricity demand at the specified node, and measured in t/MWh (t stands for tons of carbon equivalent). The *shadow carbon intensity* of a transmission constraint is defined as the system-wide reduction in carbon emissions due to an infinitesimal increase in the rating of that transmission constraint.

This paper also provides a detailed engineering and mathematical analysis of marginal CO₂ emissions in constrained power networks, derives expressions for the computation of the metrics mentioned above, and establishes relations between them. The derivations are similar to those in [8], [9], the main differences being that the focus is on emissions sensitivities, instead of losses or prices, and that the DC model of the transmission network is employed, due to its wide use by market operators in the U.S. Numerical results on a 3-bus network illustrate the high locational dependence of carbon sensitivities, and support the need for a more detailed consideration of locational effects in emission reduction policies.

The remainder of the paper is organized as follows. The next Section provides the dispatch model used in Section III to compute the marginal carbon intensities. Section IV gives relations between the nodal and

¹In the remainder of the paper, carbon and CO₂ are used interchangeably.

transmission carbon intensities. Section V analyzes the marginal carbon intensities in a 3-node network. Section VI concludes with some remarks and the Appendix includes the nomenclature.

2. Dispatch Model

Assume that the linearized lossless DC assumptions hold, so that the flows \mathbf{f} on transmission elements and flowgates are modeled by

$$\mathbf{f} = \mathbf{f}^o + \Psi(\mathbf{p} - \mathbf{p}^o - (\mathbf{1} - \mathbf{1}^o)), \quad (1)$$

where the superscript o indicates a base case power flow quantity, and \mathbf{p} and \mathbf{l} are the vectors of nodal power generation and loads, respectively. The *transmission sensitivity matrix* Ψ [10] gives the variations in flows due to changes in the nodal injections, with the reference bus assumed to ensure the real power balance. For a given point in time, the system operator dispatches the committed units to minimize the total costs of operations. Assume that the generation costs are piecewise linear, and denote the vector of nodal generation variable costs in \$/MWh by \mathbf{c} . These costs account for fuel costs \mathbf{c}_f , variable operation and maintenance costs \mathbf{c}_o , and emissions costs,

$$\mathbf{c} = \mathbf{c}_f + \mathbf{c}_o + \mathbf{R}_e \mathbf{c}_e. \quad (2)$$

The matrix \mathbf{R}_e gives the emissions rates of different pollutants for each generator, and the vector \mathbf{c}_e gives the cost of emitting each pollutant per unit of emission (e.g., in the form of an emission allowance price under a cap-and-trade program).

The economic dispatch solved is a lossless linearized DC OPF that takes into account environmental costs, along the lines of the ones discussed in [11], [12],

$$\min_{\mathbf{p}} \mathbf{c}' \mathbf{p} \quad (3)$$

$$\text{s.t. } \mathbf{1}' \mathbf{p} = \mathbf{1}' \mathbf{l} \leftrightarrow \lambda \quad (4)$$

$$\underline{\mathbf{f}} \leq \Psi(\mathbf{p} - \mathbf{l}) \leq \bar{\mathbf{f}} \leftrightarrow \underline{\boldsymbol{\mu}}, \bar{\boldsymbol{\mu}} \quad (5)$$

$$\underline{\mathbf{p}} \leq \mathbf{p} \leq \bar{\mathbf{p}} \leftrightarrow \underline{\boldsymbol{\gamma}}, \bar{\boldsymbol{\gamma}}. \quad (6)$$

Constraint (4) ensures the load-generation balance, (5) enforces the flow limits on transmission elements, and (6) models the lower and upper generation limits. The lower flow limits typically enforce flow limitations in the negative flow direction. Note that the base power flow quantities from (1) are included in the limits in (5), for notational simplicity. The nodal prices are given by

$$\boldsymbol{\pi} = -(\lambda \mathbf{1} + \Psi'(\bar{\boldsymbol{\mu}} - \underline{\boldsymbol{\mu}})). \quad (7)$$

The Lagrangian for (3)-(6) is

$$\begin{aligned} \mathcal{L} = & \mathbf{c}' \mathbf{p} + \lambda(\mathbf{1}' \mathbf{p} - \mathbf{1}' \mathbf{l}) \\ & + \underline{\boldsymbol{\mu}}'(\underline{\mathbf{f}} - \Psi(\mathbf{p} - \mathbf{l})) + \bar{\boldsymbol{\mu}}'(\Psi(\mathbf{p} - \mathbf{l}) - \bar{\mathbf{f}}) \\ & + \underline{\boldsymbol{\gamma}}'(\underline{\mathbf{p}} - \mathbf{p}) + \bar{\boldsymbol{\gamma}}'(\mathbf{p} - \bar{\mathbf{p}}). \end{aligned} \quad (8)$$

The solution of (3)-(6) satisfies the Karush-Kuhn-Tucker conditions [13], which are

$$\frac{\partial \mathcal{L}}{\partial \mathbf{p}} = \mathbf{c}' + \lambda \mathbf{1}' + (\bar{\boldsymbol{\mu}} - \underline{\boldsymbol{\mu}})' \Psi + \bar{\boldsymbol{\gamma}}' - \underline{\boldsymbol{\gamma}}' = \mathbf{0}, \quad (9)$$

together with the complementary slackness conditions for (5) and (6).

The *marginal units* are those that may change their output at an optimal redispatch in response to a small variation of a system parameter. They consist of the units that are dispatched between their generating limits, and of those that are at the limit but with the corresponding dual variables $\bar{\boldsymbol{\gamma}}$ and $\underline{\boldsymbol{\gamma}}$ equal to 0. These units have their nodal prices equal to their costs, by (7), (9). We denote the cost vector for the marginal units by $\tilde{\mathbf{c}}$ and the generation vector for marginal units by $\tilde{\mathbf{p}}$.

3. Sensitivities Computation

The objective of this section is to compute the sensitivity of a differentiable function $E(\mathbf{p})$ of the generation dispatch with respect to changes in a parameter s of (3)-(6). An example of a varied parameter is the load level at a given node in (4). The sensitivity is to be evaluated at the dispatch that solves (3)-(6). Differentiating,

$$\frac{dE}{ds} = \frac{\partial E}{\partial \mathbf{p}} \frac{d\mathbf{p}}{ds}. \quad (10)$$

The gradient $\partial E / \partial \mathbf{p}$ is easily obtained once E is specified and the solution of (3)-(6) is known. The computation of the sensitivity $d\mathbf{p} / ds$ at the optimal dispatch is discussed next.

In this section, assume that the solution of (3)-(6) exists and is unique,² that the solution of the dual problem to (3)-(6) exists and is unique as well,³ and that the optimal values of the dual variables for all binding inequality constraints are non-zero.⁴ Consider a differential change ds in a parameter of (3)-(6).

²Uniqueness rules out cases such as the existence of multiple marginal generators at the same bus. These cases are discussed in Section V.C.

³Existence and uniqueness of the dual problem solution implies a non-empty feasible set for the differential redispatch problems discussed next. Alternatively, one could assume regularity of the primal problem solution, i.e., the gradients of the binding constraints are linearly independent.

⁴This *strict complementary slackness* assumption ensures that differential perturbations will not change the set of binding inequality constraints.

To accommodate this differential change, the system operator uses the solution of (3)-(6) and solves a differential redispatch to correct for the parameter change. Under the assumptions stated above, the solutions of the primal and dual problems are continuous functions of the parameter in a neighborhood of its base case value. Hence, since the parameter change is infinitely small and the dual variables for the binding inequality constraints are non-zero, the inequality constraints that do not bind in (3)-(6) would not bind in the redispatch, and the inequality constraints that bind in (3)-(6) would bind in the redispatch. In particular, the parameter change results in dispatch changes for the marginal generators only, i.e., $d\mathbf{p}_g$ is nonzero only if generator g is marginal.

In the remainder of the paper we focus on sensitivities of the system-wide carbon emissions $E(\mathbf{p})$. However, mathematically all results hold for sensitivities of any differentiable function of generation by-products, as long as its gradient $\partial E/\partial \mathbf{p}$, is a fixed vector given the optimal dispatch. Let

$$\mathbf{r} = \left(\frac{\partial E}{\partial \mathbf{p}} \right)' \quad (11)$$

be the vector of generator carbon emission rates, in t/MWh. As a reference, the carbon emission rate is 0 t/MWh for non-fossil fuel generators and approximately 0.4 t/MWh for gas-fired combined cycle generators with a heat rate of 7000 Btu/kWh, 0.6 t/MWh for gas-fired simple cycle generators with a 11000 Btu/kWh heat rate and 0.9 t/MWh for coal-fired generators with a heat rate of 9500 Btu/kWh. These were obtained by multiplying the average carbon content of the corresponding fuel by the fuel's average energy content and the typical power plant efficiency. In the following subsections, (10) and (11) will be applied to the computation of marginal nodal carbon intensities, carbon components of locational marginal prices, and shadow carbon intensities of transmission constraints.

3.1. Differential Parameter Perturbations

Consider a differential increment dl_n in the load at a specified node n .⁵ As discussed in the previous paragraph, a differential change in load brings a differential change in the dispatch of the marginal generators only. Moreover, since the line limits and the binding constraints do not change, the flows on the binding lines also do not change. Let us denote the change in the dispatch of marginal generators by $d\tilde{\mathbf{p}}$ and construct the reduced sensitivity column vector ψ_n and reduced

⁵Or, equivalently, a differential increment $-dl_n$ in the node n generation.

sensitivity matrix $\tilde{\Psi}$ consisting of the elements of Ψ which contain the impact of injections at node n and at the marginal generator buses, respectively on binding constraints. Using these reduced matrices, we can formulate the optimization problem that is solved for the redispatch as

$$\min_{d\tilde{\mathbf{p}}} \tilde{\mathbf{c}}' d\tilde{\mathbf{p}} \quad (12)$$

$$\text{s.t. } \mathbf{1}' d\tilde{\mathbf{p}} = dl_n \leftrightarrow \tilde{\lambda} \quad (13)$$

$$\begin{bmatrix} \psi_n, \tilde{\Psi} \end{bmatrix} \begin{bmatrix} -dl_n \\ d\tilde{\mathbf{p}} \end{bmatrix} = \mathbf{0} \leftrightarrow \tilde{\boldsymbol{\mu}}. \quad (14)$$

The differential redispatch problem (12)-(14) is feasible, since the optimal value of the dual variables for (3)-(6) exists. Moreover, since the solution of (3)-(6) is unique, and the optimal values of the dual variables for all binding inequality constraints are non-zero and are continuous functions of the varied parameter it is easy to demonstrate that the solution of (12)-(14) is also unique.

The Lagrangian for (12)-(14) is

$$\tilde{\mathcal{L}} = \tilde{\mathbf{c}}' d\tilde{\mathbf{p}} + \tilde{\lambda}(\mathbf{1}' d\tilde{\mathbf{p}} - dl_n) + \tilde{\boldsymbol{\mu}}' [\psi_n, \tilde{\Psi}] [-dl_n, d\tilde{\mathbf{p}}]'. \quad (15)$$

The optimal solution for (12)-(14) satisfies

$$\frac{\partial \tilde{\mathcal{L}}}{\partial d\tilde{\mathbf{p}}} = \tilde{\mathbf{c}}' + \tilde{\lambda} \mathbf{1}' + \tilde{\boldsymbol{\mu}}' \tilde{\Psi} = 0. \quad (16)$$

From (16), we obtain that the nodal prices at the marginal generators' buses do not change with the differential change in load. The necessary condition for optimality is also sufficient in this case, since the objective function and the constraints are linear, and therefore convex [13]. Due to the strict complementary slackness assumption, (16) is satisfied for every differential perturbation $d\tilde{\mathbf{p}}$. Thus, given the uniqueness of the solution of (12)-(14) we obtain that the feasible set has only one element, and that is the (unique) solution of

$$\begin{bmatrix} \mathbf{1}' \\ \tilde{\Psi} \end{bmatrix} \frac{d\tilde{\mathbf{p}}}{dl_n} = \begin{bmatrix} 1 \\ \psi_n \end{bmatrix}, \quad (17)$$

where (17) was obtained by a rearrangement of (13)-(14). As a consequence, we conclude that the number of marginal generators is equal to the number of binding transmission constraints plus one. The change $d\tilde{\mathbf{p}}$ in generation leads to an increase in generation cost of $\tilde{\mathbf{c}}' d\tilde{\mathbf{p}} = \pi_n dl_n$. Existence of the optimal solution necessarily guarantees that the matrix in the left hand side in (17) can be inverted.

Result 1: (marginal nodal carbon intensity of a bus) From (10), (11) and (17), one can define the marginal nodal carbon intensity κ_n of bus n , in t/MW,

as

$$\kappa_n = \frac{dE}{dl_n} = \tilde{\mathbf{r}}' \frac{d\tilde{\mathbf{p}}}{dl_n} = \tilde{\mathbf{r}}' \begin{bmatrix} \mathbf{1}' \\ \tilde{\Psi} \end{bmatrix}^{-1} \begin{bmatrix} 1 \\ \psi_n \end{bmatrix}, \quad (18)$$

where $\tilde{\mathbf{r}}$ is the vector of carbon emission rates for the marginal generators. ■

The marginal carbon intensity of a given node reflects the change in system-wide carbon emissions in response to an infinitesimal change in demand at that node.

Result 2: (marginal carbon component of nodal prices) Denote the per ton carbon cost by c^c , assumed to be uniform across the system. The carbon component π_n^c of the nodal price of bus n is

$$\pi_n^c = c^c \kappa_n. \quad (19)$$

■

Although the per ton cost of carbon is constant for the entire system, the per MWh value of carbon emission varies among nodes in proportion to the nodal marginal carbon intensity.

3.2. Differential Change in Line Rating

Now consider a differential increment df_ℓ in the line rating of a specified binding line ℓ . Assume that the limit for line ℓ binds in the positive direction. As before, the differential change in line rating brings a differential change in the dispatch of the marginal generators only, and the flows on the binding lines do not change, except for the flow on line ℓ , which increases exactly by df_ℓ . Proceeding as in the previous subsection, denote the change in the dispatch of the marginal units by $d\tilde{\mathbf{p}}$, and construct the reduced transmission sensitivity row vector $\tilde{\psi}_\ell$ and matrix $\tilde{\Psi}_{-\ell}$ consisting of flow sensitivities for the line ℓ and for the rest of the flow elements with binding limits, respectively, with respect to injections at the marginal generator buses. The optimization problem that is solved for the redispatch is

$$\min_{d\tilde{\mathbf{p}}} \tilde{\mathbf{c}}' d\tilde{\mathbf{p}} \quad (20)$$

$$\text{s.t. } \mathbf{1}' d\tilde{\mathbf{p}} = 0 \quad \leftrightarrow \quad \tilde{\lambda} \quad (21)$$

$$\tilde{\psi}_\ell d\tilde{\mathbf{p}} = df_\ell \quad \leftrightarrow \quad \tilde{\mu}_\ell \quad (22)$$

$$\tilde{\Psi}_{-\ell} d\tilde{\mathbf{p}} = \mathbf{0} \quad \leftrightarrow \quad \tilde{\boldsymbol{\mu}}_{-\ell}. \quad (23)$$

Using the same argument as in the previous section, one concludes that the feasible set of (20)-(23) has only one element, and that is the (unique) solution of

$$\begin{bmatrix} \mathbf{1}' \\ \tilde{\psi}_\ell \\ \tilde{\Psi}_{-\ell} \end{bmatrix} \frac{d\tilde{\mathbf{p}}}{df_\ell} = \begin{bmatrix} 0 \\ 1 \\ \mathbf{0} \end{bmatrix}, \quad (24)$$

where (24) was obtained by a rearrangement of (21)-(23). The change $d\tilde{\mathbf{p}}$ in generation leads to an increase in generation cost of $\tilde{\mathbf{c}}' d\tilde{\mathbf{p}} = -\bar{\mu}_\ell df_\ell$.

The case in which the constraint for line ℓ binds in the negative direction is similar, and $d\tilde{\mathbf{p}}/df_\ell$ is the unique solution of

$$\begin{bmatrix} \mathbf{1}' \\ \tilde{\psi}_\ell \\ \tilde{\Psi}_{-\ell} \end{bmatrix} \frac{d\tilde{\mathbf{p}}}{df_\ell} = \begin{bmatrix} 0 \\ -1 \\ \mathbf{0} \end{bmatrix}. \quad (25)$$

The above discussion leads to the following:

Result 3: (shadow carbon intensity of transmission constraints) Denote the shadow carbon intensities of increasing the maximum and minimum capacities of transmission line ℓ by $\bar{\mu}_\ell^c$ and $\underline{\mu}_\ell^c$, respectively. Then,

$$\bar{\mu}_\ell^c = -\tilde{\mathbf{r}}' \frac{d\tilde{\mathbf{p}}}{df_\ell} = \begin{cases} -\tilde{\mathbf{r}}' \begin{bmatrix} \mathbf{1}' \\ \tilde{\psi}_\ell \\ \tilde{\Psi}_{-\ell} \end{bmatrix}^{-1} \begin{bmatrix} 0 \\ 1 \\ \mathbf{0} \end{bmatrix} & \text{if } \bar{\mu}_\ell > 0 \\ 0 & \text{otherwise,} \end{cases} \quad (26)$$

and

$$\underline{\mu}_\ell^c = -\tilde{\mathbf{r}}' \frac{d\tilde{\mathbf{p}}}{df_\ell} = \begin{cases} -\tilde{\mathbf{r}}' \begin{bmatrix} \mathbf{1}' \\ \tilde{\psi}_\ell \\ \tilde{\Psi}_{-\ell} \end{bmatrix}^{-1} \begin{bmatrix} 0 \\ -1 \\ \mathbf{0} \end{bmatrix} & \text{if } \underline{\mu}_\ell > 0 \\ 0 & \text{otherwise.} \end{cases} \quad (27)$$

■

The negative signs in (26) and (27) are introduced to be consistent with the standard definition of economic shadow prices in a cost-minimization framework, i.e., the negative of the corresponding sensitivities.⁶

4. Relations Between Nodal and Transmission Shadow Carbon Intensities

Denote the reference bus by $n = 0$ and the carbon intensity at the reference bus by $-\lambda^c$. By the definition of the transmission sensitivity matrix, $\psi_0 = \mathbf{0}$. Hence,

$$-\lambda^c = \kappa_0 = \tilde{\mathbf{r}}' \begin{bmatrix} \mathbf{1}' \\ \tilde{\Psi} \end{bmatrix}^{-1} \begin{bmatrix} 1 \\ \mathbf{0} \end{bmatrix}. \quad (28)$$

⁶The shadow price for a constraint is the Lagrange multiplier of the constraint [14]. In cost-minimization problems, the optimal Lagrange multiplier for a constraint is the negative of the sensitivity of the objective function with respect to a variation in the constraint limit [13].

Consider now the carbon intensity κ_n for node n ,

$$\begin{aligned}
\kappa_n &= \tilde{\mathbf{r}}' \begin{bmatrix} \mathbf{1}' \\ \tilde{\Psi} \end{bmatrix}^{-1} \begin{bmatrix} 1 \\ \psi_n \end{bmatrix} \\
&= \tilde{\mathbf{r}}' \begin{bmatrix} \mathbf{1}' \\ \tilde{\Psi} \end{bmatrix}^{-1} \begin{bmatrix} 1 \\ \mathbf{0} \end{bmatrix} \\
&\quad + \sum_{\ell, \underline{\mu}_\ell > 0} \psi_{\ell n} \tilde{\mathbf{r}}' \begin{bmatrix} \mathbf{1} \\ \tilde{\psi}_\ell \\ \tilde{\Psi}_{-\ell} \end{bmatrix}^{-1} \begin{bmatrix} 0 \\ 1 \\ \mathbf{0} \end{bmatrix} \\
&\quad - \sum_{\ell, \underline{\mu}_\ell < 0} \psi_{\ell n} \tilde{\mathbf{r}}' \begin{bmatrix} \mathbf{1} \\ \tilde{\psi}_\ell \\ \tilde{\Psi}_{-\ell} \end{bmatrix}^{-1} \begin{bmatrix} 0 \\ -1 \\ \mathbf{0} \end{bmatrix} \\
&= -\left(\lambda^c + \sum_{\ell} \psi_{\ell} (\bar{\mu}_\ell^c - \underline{\mu}_\ell^c) \right). \tag{29}
\end{aligned}$$

Expression (29) can be summarized as:

Result 4: (relation between marginal nodal carbon intensity and shadow carbon intensity of transmission lines) Construct the vectors $\boldsymbol{\kappa}$ of nodal carbon intensities and $\bar{\boldsymbol{\mu}}^c, \underline{\boldsymbol{\mu}}^c$ of shadow carbon intensities of transmission lines. Then,

$$\boldsymbol{\kappa} = -\left(\lambda^c \mathbf{1} + \Psi' (\bar{\boldsymbol{\mu}}^c - \underline{\boldsymbol{\mu}}^c) \right). \tag{30}$$

Note that the relation between nodal carbon intensities and shadow intensities of transmission constraints (30) has the same structure as the prices and economic transmission shadow values (7). In fact, if one were to replace $\tilde{\mathbf{r}}$ by $\tilde{\mathbf{c}}$, then (30) would be exactly (7). Since the derivation of (30) holds for every $\mathbf{r} = (\partial E / \partial \mathbf{p})'$, we conclude that the nodal intensity of any generation by-product, such as cost, carbon or renewable generation, is equal to the corresponding nodal intensity at the reference bus plus the sum of the shadow intensities of transmission constraints weighted by the corresponding elements of the transmission sensitivity matrix.

The dot product of the nodal carbon intensities (30) and the net load $(\mathbf{1} - \mathbf{p})$ gives the net *carbon congestion rent* that the system operator receives. This is the gap between the amount of carbon paid for by loads and the amount of carbon for which generators are compensated through nodal prices. This rent is related to the shadow carbon intensities of transmission lines by

$$\begin{aligned}
\boldsymbol{\kappa}' (\mathbf{1} - \mathbf{p}) &= -\left(\lambda^c \mathbf{1} + \Psi' (\bar{\boldsymbol{\mu}}^c - \underline{\boldsymbol{\mu}}^c) \right)' (\mathbf{1} - \mathbf{p}) \\
&= -(\bar{\boldsymbol{\mu}}^c - \underline{\boldsymbol{\mu}}^c)' \Psi (\mathbf{1} - \mathbf{p}) \\
&= (\bar{\boldsymbol{\mu}}^c - \underline{\boldsymbol{\mu}}^c)' \mathbf{f}. \tag{31}
\end{aligned}$$

The carbon congestion rent can be expressed in tons of carbon, or in \$ by multiplying it by the unit cost of carbon, c^c .

Table 1. 3-Bus Example: Generation Characterization

generator	$g1$	$g2$
fuel + v.o.m. costs	\$30/MWh	\$20/MWh
carbon costs	\$10/t	\$10/t
carbon emission rate	0.4 t/MWh	0.9 t/MWh
total variable cost	\$34/MWh	\$29/MWh
capacity	50 MW	30 MW

In systems with a positive carbon congestion rent, loads pay for CO₂ in the nodal prices in excess of generator receipts. This indicates that relieving transmission congestion would reduce CO₂ emissions and would thereby reduce load payments for carbon. In systems with a negative carbon congestion rent, nodal price-based load payments for CO₂ are lower than generator receipts. This shows that relieving transmission congestion in the system would increase CO₂ emissions, thus load payments for carbon would increase. The shadow carbon intensity of transmission constraints and the carbon congestion rent may be used as screening metrics to quickly identify the impact of individual transmission constraints on CO₂ emissions in the system and find congestion relief targets that would reduce carbon emissions.

5. Numerical Examples

Consider a three-bus example of an electrical network shown in Fig. 1, which includes two generators, $g1$ and $g2$, located at buses 1 and 2, respectively, and one load attached to each bus. Loads at buses 1 and 2 are small, 1 MW each. Bus 3 has the largest load, 50 MW, and no generation attached to it. Each generator is characterized by three parameters: capacity (MW), cost (\$/MWh) and CO₂ emission rate (t/MWh); the data is provided in Table 1. The cost reflects generator's fuel costs, non-fuel variable O&M expenses and the cost of CO₂ emissions computed as a product of the generator's emission rate and the price of carbon, \$10/t in this example.

Without transmission constraints and losses, the optimal dispatch utilizes the least expensive resource (generator $g2$) up to its capacity of 30 MW and meets the remaining 22 MW of demand from generator $g1$, as shown in Table 2. Generator $g1$ is the single marginal generating unit that sets the price and defines the marginal carbon intensity for all locations. Thus, the nodal prices at all buses are equal the cost of generator $g1$, \$34/MWh, and the nodal carbon intensity for all

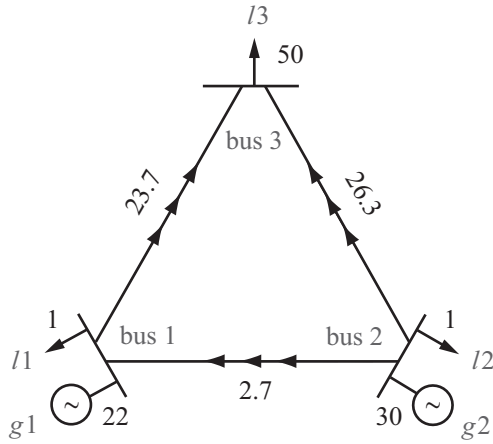


Figure 1. Unconstrained dispatch in a 3-bus network; all lines have identical impedance. Flows, generation and loads are in MW.

Table 2. 3-Bus Example: Unconstrained Case

node	1	2	3
generation MW	22	30	-
load MW	1	1	50
nodal price \$/MWh	34	34	34
marginal carbon intensity t/MWh	0.4	0.4	0.4
nodal carbon price \$/MWh	4	4	4

buses are equal to the emission rate of generator $g1$, 0.4 t/MWh. The carbon component of the nodal prices is therefore \$4/MWh for all nodes. In this example, reducing demand by 1 MWh at any location would reduce carbon emission by 0.4 t, and would save \$34 in total generation costs of which \$4 would be on account of carbon reduction. If all lines have the same impedance, the resulting flows are as shown in Fig. 1.

Consider now the case where the flow on the line 2 – 3 is limited at 20 MW, shown in Fig. 2. The unconstrained dispatch of Fig. 1 is not feasible, because it results in a flow of 26.3 MW which is above the limit. A redispatch is necessary to accommodate this constraint. The optimal dispatch and corresponding nodal prices are shown on Fig. 2 and Table 3. In this case both generating units are marginal. Nodal prices at their buses are equal to their respective offers of \$34/MWh and \$29/MWh, respectively. Indeed, the only way to serve an incremental MW of demand at bus 1 is to dispatch generator $g1$, because any attempt to obtain any portion of that power from generator $g2$ would increase the flow over line 2 – 3 and violate the constraint. The least expensive way to serve an

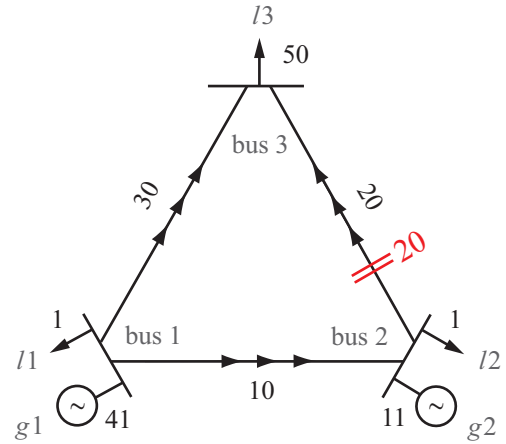


Figure 2. Constrained dispatch in a 3-bus network; all lines have identical impedance.

Table 3. 3-Bus Example: Constrained Case

node	1	2	3
generation MW	41	11	-
load MW	1	1	50
nodal price \$/MWh	34	29	39
marginal carbon intensity t/MWh	0.4	0.9	-0.1
nodal carbon price \$/MWh	4	9	-1

incremental demand at bus 2 is to ramp up unit $g2$. However, to serve an incremental MW at bus 3 without violating the transmission constraint 2 – 3, it would be necessary to increase generation at $g1$ by 2 MW and reduce the output of generator $g2$ by 1 MW. Hence the cost of serving that incremental demand is \$39/MWh = 2 x \$34/MWh - 1 x \$29/MWh.

The same logic is applicable for computing locational marginal carbon emission rates. Since incremental load at bus 1 is served by unit $g1$, the marginal carbon intensity at this bus is 0.4 t/MWh, the emission rate of $g1$. An incremental load at bus 2 is served by unit $g2$ and its marginal carbon intensity is 0.9 t/MWh. As explained earlier, to serve an incremental load at bus 3 it is necessary to increase generation at bus 1 by 2 MW and reduce generation at bus 2 by 1 MW. The result of this redispatch action would be an increase of carbon emissions at bus 1 by 2 x 0.4 t/MWh and a reduction of carbon emissions at bus 2 by 0.9 t/MWh adding up to an overall 0.1 t/MWh reduction in carbon emissions. Thus, the marginal carbon intensity at bus 3 is -0.1 t/MWh.

Given these results we conclude that demand reduction at buses 1 and 2 would cause a reduction in

carbon emissions but demand reduction at bus 3 would actually increase carbon emissions despite the fact that this location has the highest demand and highest prices in the system and therefore is the most attractive target of a demand response program. Although a demand response program may make most economic sense, it would not reduce carbon emissions but increase them (this example is consistent with [15], where a statistical analysis of demand reduction measures relying on real-time prices indicates that demand reduction could result in an increase in emissions, in this case NO_x and SO_2).

Consider the addition of 1 MW of carbon-free wind generation to the system. Assuming zero operating costs of wind power, this generation addition can be modeled as a 1 MW reduction in demand. Wind addition to buses 1 or 2 would reduce carbon emissions by 0.4 t or 0.9 t, respectively. However, the addition of carbon free wind generation at bus 3 would increase total carbon emissions by 0.1 t.

The counter-intuitive results obtained at bus 3 are due to transmission congestion along the line 2 – 3, which ramps down unit g_2 with a high carbon emission rate. This congestion appears to be “good” from the emissions point of view and indirect attempts to relieve the constraint by reducing demand or adding supply at bus 3 would reduce dispatch costs but increase emissions. This can be confirmed by the calculation of the shadow carbon intensity of constraint 2 – 3. Indeed, increasing the rating of this constraints by 1 MW would allow to increase a dispatch of unit g_2 by 3 MW while reducing by 3 MW dispatch of unit g_1 . Doing so will reduce dispatch costs by $-\$15 = 3 \times \$29 - 3 \times \$34$ but will increase carbon emissions by $1.5 \text{ t} = 3 \times 0.9 \text{ t} - 3 \times 0.4 \text{ t}$. In other words, the shadow carbon intensity of constraint 2–3 is -1.5. If the reference node is bus 3, the relation between nodal carbon intensities and transmission shadow intensities can be verified by

$$\begin{aligned} \kappa &= \begin{bmatrix} 0.4 \\ 0.9 \\ -0.1 \end{bmatrix} \\ &= \begin{bmatrix} -0.1 \\ -0.1 \\ -0.1 \end{bmatrix} + \begin{bmatrix} 1/3 & 2/3 & 1/3 \\ -1/3 & 1/3 & 2/3 \\ 0 & 0 & 0 \end{bmatrix} \begin{bmatrix} 0 \\ 0 \\ 1.5 \end{bmatrix} \quad (32) \end{aligned}$$

The carbon congestion rent is -30 t, or -\$300, which indicates that relieving congestion increases carbon emissions.

Note that the results are not absolute and depend on the underlying price of carbon emissions. Currently, fossil-fueled generation costs are dominated by fuel costs. Thus, the cost minimizing dispatch essentially minimizes the costs of fuel. If carbon costs increase so that they begin to affect the generation merit order,

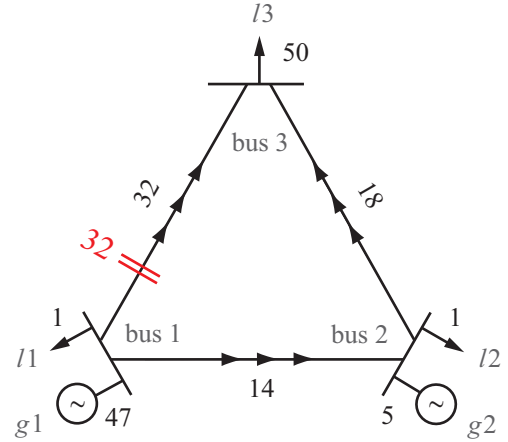


Figure 3. Constrained dispatch in a 3-bus network; high carbon cost case.

prices and marginal nodal carbon intensities would show a higher correlation.

To illustrate that, consider the case with an increased carbon cost of \$30/t, and let the limit on line 1 – 3 be 32MW. The total variable costs are then \$42/MWh for g_1 and \$47/MWh for g_2 . This change in carbon costs changes the merit order: now g_1 has lower costs than g_2 , as opposed to the case with \$10/t carbon cost. As a result, the dispatch changes such that line 2 – 3 is no longer constrained, but line 1 – 3 operates at its maximum rating of 32 MW. The solution is shown in Fig. 3 and Table 4. The price at bus 3 is \$58/MWh, since a 1 MW increase in load at bus 3 causes g_1 to decrease generation by 1 MW and g_2 to increase generation by 2 MW. Hence, the increase in total emissions due to the load increment at bus 3 is 1.4 t/MWh, compared to -0.1 t/MWh with the low carbon cost case. Note that in this case the increase in the carbon cost made the carbon intensity at node 3 positive. Thus, a change in the carbon price made node 3 the best place for a load reduction program that aims to reduce emissions. Before the price increment, the bus 3 was the worst place to conserve energy with the objective of reducing emissions. The carbon congestion rent is +48 t, or \$1440, which indicates that relieving congestion decreases carbon emissions.

The examples on the 3-bus test system in this section illustrate the importance of locational effects in marginal carbon intensities. In actual systems, negative marginal carbon intensities may or may not occur, depending on the transmission topology, the congestion patterns and the resource mix. Studies of actual system are underway, and their results will be presented in future papers.

Table 4. 3-Bus Example: High Carbon Cost, Constrained Case

node	1	2	3
generation MW	47	5	–
load MW	1	1	50
nodal price \$/MWh	42	47	52
marginal carbon intensity t/MWh	0.4	0.9	+1.4
nodal carbon price \$/MWh	12	27	+4.2

6. Concluding Remarks

This paper defines marginal nodal and transmission line carbon intensities, and develops a mathematical approach for their analysis and computation. The approach is general and can be applied to the calculation of sensitivities of other functions of the generation dispatch, such as SO_x and NO_x emissions, natural gas consumption, renewable power use, and generation costs. If the generation costs are used, the sensitivities match the widely employed nodal prices and shadow transmission prices. We show that the relations between nodal and transmission shadow prices hold for all such sensitivities, not just for cost sensitivities. The approach requires a low computational effort, as only a very small matrix of dimension the number of binding constraints is factorized.

The computation of marginal carbon intensities in a 3-bus network yielded many insights. Given the wide spectrum of emission rates, the nodal carbon intensities can show significant variations from node to node. Moreover, nodal carbon intensities can be positive or negative at buses with no marginal generators. Negative carbon intensities mean that small load reductions increase system-wide carbon emissions. This counterintuitive effect may occur even at nodes with the highest prices, and is due to transmission congestion.

The locational nature of carbon intensities and their large range of variation have deep implications on how renewable portfolio standards, demand reduction programs, transmission developments and electricity market design impact carbon emissions. In general, carbon policies that do not account for locational effects may not be effective in attaining their goals. The work in this paper is being applied to the analysis of the power network effects on carbon emissions in the U.S. taking full account of commitment and dispatch decisions. The results from these studies will help develop effective policies for carbon emissions reductions.

Appendix Nomenclature

o : related to the base case power flow,
 c : related to carbon,
 \sim : related to marginal units,
 $^+$: upper limit,
 $^-$: lower limit,
 n : bus index,
 ℓ : line index,
 g : generator index,
 s : an arbitrary parameter,
 c : cost,
 \mathbf{c} : vector of generation cost,
 \mathbf{r} : vector of generation emission rates,
 $\mathbf{0}$: vector of zeros,
 $\mathbf{1}$: vector of ones,
 \mathbf{p} : vector of generation,
 \mathbf{l} : vector of loads,
 \mathbf{f} : vector of flows on transmission elements,
 \mathbf{e} : vector of generation carbon emissions,
 E : total generation carbon emissions,
 Ψ : transmission sensitivity matrix,
 ψ : an element of Ψ ,
 λ : shadow price of the supply-demand constraint,
 μ : shadow price of transmission limits,
 γ : shadow price of generation limits,
 π : nodal price of energy,
 κ : nodal carbon intensity.

References

- [1] P. Lindstrom, "Emissions of greenhouse gases report," Energy Information Administration, Washington, DC, Report DOE/EIA-0573, Chap. 2, Dec. 2008. [Online]. Available: <http://www.eia.doe.gov/environment>
- [2] A. Schwarzenegger, Exec. Order S-14-08, Office of the Governor of the State of California, Sacramento, CA, Nov. 2008. [Online]. Available: <http://gov.ca.gov/executive-order/11072/>
- [3] The Regional Greenhouse Gas Initiative, Inc. New York, NY. [Online]. Available: <http://www.rggi.org>
- [4] R. J. Spiegel, D. L. Greenberg, E. C. Kern, and D. E. House, "Emissions reduction data for grid-connected photovoltaic power systems," *Solar Energy*, vol. 68, no. 5, pp. 475–485, May 2000.
- [5] R. Bettle, C. Pout, and E. Hitchin, "Interactions between electricity-saving measures and carbon emissions from power generation in England and Wales," *Energy Policy*, vol. 34, no. 18, pp. 3434–3446, Dec. 2006.
- [6] M. Grubb and K. Neuhoff, "Allocation and competitiveness in the EU emissions trading scheme: policy overview," *Climate Policy*, vol. 6, no. 1, pp. 7–30, 2006.
- [7] Y. Chen, J. Sijm, B. F. Hobbs, and W. Lise, "Implications of CO₂ emissions trading for short-run electricity market outcomes in northwest Europe," *Jour. Regul. Econ.*, vol. 34, no. 3, pp. 251–281, Dec. 2008.
- [8] P. R. Gribik, D. Shirmohammadi, S. Hao, and C. L. Thomas,

- “Optimal power flow sensitivity analysis,” *IEEE Trans. Power Syst.*, vol. 5, no. 3, pp. 969–976, Aug. 1990.
- [9] A. J. Conejo, E. Castillo, R. Mínguez, and F. Milano, “Locational marginal price sensitivities,” *IEEE Trans. Power Syst.*, vol. 20, no. 4, pp. 2026–2033, Nov. 2005.
- [10] X. Cheng and T. J. Overbye, “An energy reference bus independent LMP decomposition algorithm,” *IEEE Trans. Power Syst.*, vol. 21, no. 3, pp. 1041–1049, Aug. 2006.
- [11] J. K. Delson, “Controlled emission dispatch,” *IEEE Trans. Power App. Syst.*, vol. PAS-93, no. 5, pp. 1359–1366, Sept./Oct. 1974.
- [12] J. H. Talaq, F. El-Hawary, and M. E. El-Hawary, “A summary of environmental/economic dispatch algorithms,” *IEEE Trans. Power Syst.*, vol. 9, no. 3, pp. 1508–1516, Aug. 1994.
- [13] D. P. Bertsekas, *Nonlinear Programming*, 2nd ed. Belmont, MA: Athena Scientific, 1999.
- [14] A. Mas-Colell, M. D. Whinston, and J. R. Green, *Microeconomic Theory*. Ney York, NY: Oxford University Press, 1995.
- [15] S. P. Holland and E. T. Mansur, “The short-run effects of time-varying prices in competitive electricity markets,” *Energy Jour.*, vol. 27, no. 4, pp. 127–155, 2006.